Materials Characterization 145 (2018) 65–76

Contents lists available at ScienceDirect

Materials Characterization

journal homepage: www.elsevier.com/locate/matchar

Fractal analysis of Mo and Nb effects on grain boundary character and hot cracking behavior for Ni-Cr-Fe alloys

Xiao Wei[a], Mengjia Xu[b], Jingqing Chen[c], Chun Yu[a], Junmei Chen[a], Hao Lu[a,*], Jijin Xu[a,*]

[a] Shanghai Key Lab of Shanghai Laser Manufacturing and Materials Modification, School of Materials Science and Engineering, Shanghai Jiao Tong University, Shanghai 200240, China
[b] School of Mechanical Engineering, Shanghai Dianji University, Shanghai 201306, China
[c] School of Materials Science and Engineering, Southwest Jiao Tong University, Chengdu 611756, China

ARTICLE INFO

Keywords:
Ni-based alloy
Polycrystalline deformation
GROD
Ductility-dip cracking
Fractal analysis

ABSTRACT

In this paper, two filler metals of alloy 690 were evaluated on their hot cracking resistance based on the fractal analysis of random high-angle grain boundary (RHGB) morphologies. A grain reference orientation deviation (GROD) map based on EBSD technique was conducted to investigate the polycrystalline strain distribution on different RHGB network. It was found that for the 52M weld metal, specimen from the cross section with straight dendritic GBs exhibited lower fractal dimension, showing higher DDC susceptibility than the specimen from the surface section with higher fractal dimension due to equiaxed grains with tortuous GBs. With Mo and more Nb adding to the filler metal 52MSS, smaller grains nucleated and fractal dimension of the RHGB network increased, thus the cracking resistance was greatly improved. The GROD results revealed that local strain commonly concentrated around RHGB at high temperatures, especially near long and straight RHGB. The dense and tortuous RHGB network, resulting in the higher fractal dimension, could bear a more uniform strain distribution and balance the deformation between GB and grains, leading to better performance on cracking resistance. Moreover, dynamic recrystallized grains were observed beside GBs and their amount increases where there was cracking at 1050 °C, especially for the 52MSS. As a result, crack propagation path was blocked and fractal dimension increased as well.

1. Introduction

Alloy 690 is a Ni-Cr-Fe type alloy with excellent performances at high temperatures and has been widely applied to pipeline welding of nuclear power application. During fabrication of nuclear core equipment, welding is an essential process to assemble various pipelines and tubes, which are often subjected to complex combination of severe thermal and mechanical conditions. However, the reheated weld and heat affected zone (HAZ) of alloy 690 weldments were found susceptible to intergranular hot cracking, referred as ductility-dip cracking (DDC), in high restraint manufacturing conditions, such as narrow gap welding, which seriously affects the security and service life in nuclear application [1–3]. A Gleeble-based hot tensile test was devised by Nissley et al. [4,5] to investigate the reason of the cracking, referred to as strain-to-fraction (STF) test. Based on the results, several hypotheses have been proposed to describe cracking mechanisms, including intergranular precipitation, grain boundary (GB) sliding, impurity element embrittlement [6–16].

According to GB sliding mechanism, ductility-dip cracking of alloy 690 and the companion filler metal was well explained by a creep-like phenomenon. GB with approximate 45° to loading was found to prone to sliding but cracking propagation most preferentially occurred on GB vertical to loading [3,17,18]. Many efforts had been taken to reinforce GB strength, such as impurity elements control and rare earth elements addition [6,19–24]. In another hypothesis, the interdendritic precipitation of M(C,N) was believed having an positive effect by pinning the migration of GB [2,25]. With Mo and Nb addition into the composition of filler metal, Laves phase (enriched with Ni, Nb) and (Nb, Ti)C were precipitated at the end of solidification to acquire a much tortuous GB morphology. The weld metal exhibited better mechanical strength [19,24,26] and the microstructure was found free of DDC during welding condition [26–28]. It was apparent that the GB morphology influenced the high temperature performance of filler metal and resistance of DDC. However, the precise effect of tortuous GB character on DDC remained unclear and quantification.

In the weld metal of alloy 690, variations in the GB morphology can

* Corresponding authors.
E-mail addresses: shweld@sjtu.edu.cn (H. Lu), xujijin_1979@sjtu.edu.cn (J. Xu).

https://doi.org/10.1016/j.matchar.2018.08.024
Received 26 June 2018; Received in revised form 15 August 2018; Accepted 15 August 2018
Available online 17 August 2018
1044-5803/

Table 1
Chemical compositions of the two filler metals wt%.

Material	Ni	Cr	Fe	Mn	Ti	Al	P	S	C	Nb	Mo
FM-52M	Bal.	30.06	8.22	0.8	0.224	0.11	0.003	0.001	0.02	0.84	–
FM-52MSS	Bal.	30.18	8.2	0.8	0.2	0.07	0.003	0.001	0.02	2.48	4.0

be observed according to position of joint. To analyze the cracking resistance correlative to GB character, STF tests were conducted on two filler metals of alloy 690. Fractal analysis was implemented to quantitatively determinate the relevance between the grain boundary tortuousness and DDC susceptibility. Grain reference orientation deviation (GROD) based on EBSD technique was applied to analyze intra- and inter-granular strain distribution. Combined with JmatPro calculation, the precipitation behavior in filler metal with Mo and Nb addition and its effect on the tortuous GB character were explained.

2. Materials and Methods

The materials used in this work were two commercial filler metal: FM-52M and FM-52MSS. The chemical compositions of two filler metals are listed in Table 1. FM-52MSS contains 1.6 wt% Nb and 4.0wt% Mo more than FM-52M.

At first, GTAW was performed on low carbon steel with 1.2 mm filler wire. The schematic illustration of welding joint was shown in Fig. 1a. To avoid solute dilution, a 4 mm thick of overlay was deposited on low carbon steel in advance. The GTAW was performed under the welding parameters: current 180 A (150–220 A), arc voltage 13 V (11–14 V), welding speed 2 mm s^{-1} and preheating temperature 50 °C. Finally, an approximate 100 mm weldment was completed.

Once the welding completed, STF specimens were directly cut to the final dimensions by wire electro-discharge, as shown in Fig. 1b and c. According to the position of joint, two kinds of specimens were fabricated: one was cut from the upper surface of joint (A specimen in the Fig. 1b); the other was cut from the cross section of the joint (B specimen in the Fig. 1b). Surfaces of the specimens were ground till 800# abrasive paper and one side was ground till 2000# abrasive paper, and then polished with 1.0–0.5 μm SiC particles. Each specimen was marked by microhardness indenter with 0.5 mm interval (within 4 mm of center), as shown in Fig. 1c. The marks were used to record the local strain distribution after test. Due to limited materials, FM-52M weldment was fabricated into two kinds of specimen, while FM-52MSS only had specimens parallel to weldment surface.

The STF test was conducted based on Gleeble 3500, as illustrated in Fig. 2. Specimens were heated at a rapid speed of 100 °C s^{-1} to 850 °C or 1050 °C, and held at the temperature for 10 s, to simulate the reheated welding conditions during multipass welding. Then a stroke of 1.5 to 2.0 mm at rate of 0.1 mm $s^{-1}$was loaded on the specimen and held for 10 s before cooling. During STF tests, inevitable temperature differences were generated between regions with varying distances to center, which induced larger deformation on hotter part of specimen. The temperature histories were recorded by thermocouples (2 or 3 pairs) during the tests. Based on the measured results, the temperature difference of region 2 mm from the center of specimen was about 5 °C. Half-contact stainless steel clamps were used to limit the temperature differences. Thus deformation commonly concentrated within 4 mm of center and DDC mostly occurred within 2–4 mm. A stoke rate of 0.1 mm s^{-1} was taken in this test similar to strain rate for standard STF test (0.5 mm s^{-1} to 19 mm-length reduced section).

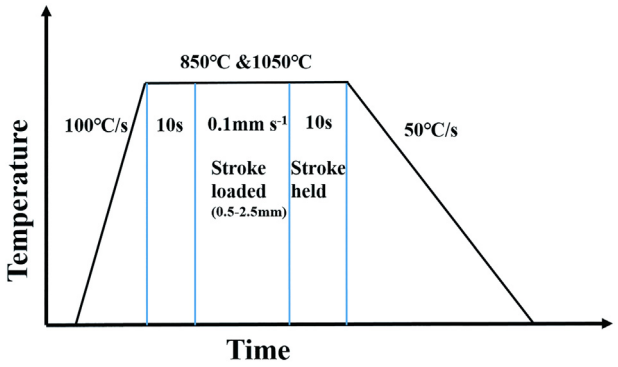

Fig. 2. Illustration of the STF procedure.

Before and after STF tests, analysis of crack morphology and local deformation were carried out by Zeiss Imager A1m optical microscope (OM) and a NOVA NanoSEM 230 scanning electron microscope (SEM). Specimens were etched by 10% chromic acid for 30 s under 4.5 V for the observation. The GB misorientation was summarized by electron backscatter diffraction (EBSD) analysis. Electrolytic polishing was conduct to remove oxidation of specimens. The electrolyte was made of 10%$HClO_4$ + 90%CH_3COOH and carried out under 15 V for 20 s. JmatPro 6.1 was used for thermal dynamical calculation to provide an understanding of precipitation behavior during solidification.

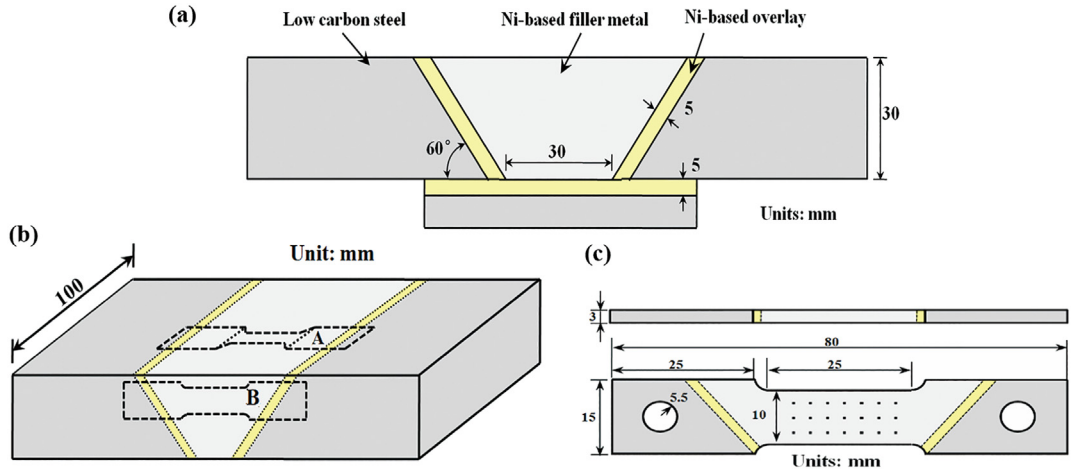

Fig. 1. Schematic illustrations of material preparation (a) weldment (b) specimen preparation (c) dimensions of the specimen.